Available online at www.sciencedirect.com
SCIENCE DIRECT®
Journal of Sound and Vibration 293 (2006) 795–806
JOURNAL OF SOUND AND VIBRATION
www.elsevier.com/locate/jsvi

Out-of-round railway wheels—assessment of wheel tread irregularities in train traffic

Anders Johansson[a,b,*]

[a]*Department of Applied Mechanics, Chalmers University of Technology, SE-412 96 Göteborg, Sweden*
[b]*Epsilon HighTech AB, Lindholmspiren 9, SE-417 56 Göteborg, Sweden*

Accepted 26 August 2005
Available online 13 February 2006

Abstract

Results from an extensive wheel measurement campaign performed in Sweden are given and discussed. Out-of-roundness (OOR), transverse profile and surface hardness of 99 wheels on passenger trains (X2 and intercity), freight trains, commuter trains (Regina) and underground trains (C20) were measured. Both tread and disc braked wheels were investigated. The selected wheels had travelled a distance of more than 100000 km, and the measurements were conducted when the train wagons/coaches had been taken out of traffic for maintenance, most of them due to reasons other than wheel OOR. Mechanical contact measurement methods were used. The highest roughness levels (higher than 20 dB re 1 μm for some wheels) were found on powered high-speed (X2) train wheels. The previously known polygonalization of C20 underground wheels is quantified. It is also verified that an initial irregularity is formed due to the clamping in a three-jaw chuck during profiling of new C20 wheels. Magnitudes and wavelength contents of measured wheel roughness are compared with corresponding measurements of rail roughness.

1. Introduction

Since there is an increasing demand for high-speed intercity and commuter train traffic, noise from railway operation is becoming an increasingly important source of annoyance in society. Freight traffic with higher train speeds also contributes to increasing noise levels. One solution to the problem is to install noise barriers. However, this is expensive and it disturbs the aesthetic impression of railways for both passengers and people living near railway lines. Research to find means of noise reduction is motivated by stricter legislation concerning allowable noise levels. At train speeds below around 250 km/h, the total railway noise level is dominated by noise generated by the dynamic wheel–rail interaction. Thus, aerodynamically generated noise plays a minor role in this speed range.

The source of railway rolling noise is vibrations induced by low amplitude, short-pitch undulations (surface roughness, waviness, corrugation) on wheel treads and rail heads. Two other types of railway noise are impact

*Corresponding author. Department of Applied Mechanics, Chalmers University of Technology, SE-412 96 Göteborg, Sweden. Tel.: +46 31 772 15 00; fax: +46 31 772 38 27.
E-mail address: anders.johansson@chalmers.se.

0022-460X/$ - see front matter
doi:10.1016/j.jsv.2005.08.048

Nomenclature

k	number of one-third octave band [dimensionless]
L_r^k	roughness level for one-third octave band k [dB re 1 μm]
$L_{r,n}^k$	roughness level for wheel number n and one-third octave band k [dB re 1 μm]
$\bar{L}_r^k$	mean roughness level for one wheel category for one-third octave band k [dB re 1 μm]
n	wheel number within one wheel category [dimensionless]
N	number of wheels within one category [dimensionless]
$r(x)$	wheel irregularity/roughness profile [m]
r_{ref}	reference value for wheel roughness [m]
$\tilde{r}_k$	root mean square value of the roughness profile [m]
$\tilde{r}_{k,\mathrm{mean}}$	mean root mean square roughness value for all wheels within one category for one-third octave band k [m]
$\tilde{r}_{k,n}$	root mean square value for wheel number n and one-third octave band k [m]
$\hat{r}(\lambda_\theta)$	amplitude of harmonic OOR order with wavelength λ_θ [m]
$\tilde{r}_\theta$	root mean square irregularity value for harmonic order θ [m]
R_0	mean wheel radius [m]
$R(x)$	wheel radius as function of circumferential coordinate [m]
x	circumferential coordinate [m]
θ	harmonic order of OOR [dimensionless]
λ_k	centre wavelength for one-third octave band k [m]
λ_θ	wavelength for θth harmonic order of the OOR [m]
φ	rotational angle around the wheel circumference [rad]

noise (generated for example by a wheel flat or by a wheel passing a rail joint) and squeal noise (generated by lateral stick-slip excitation in sharp curves). A review of the modelling of wheel–rail noise generation is given by Thompson and Jones [1]. Rolling noise covers the frequency interval 100–5000 Hz, with the highest levels in the interval 500–2500 Hz. For frequencies below 500 Hz, the main contribution to the noise is radiated by the sleepers, whereas for frequencies between approximately 500 Hz and 1–2 kHz, rail vibration is the dominating source. Stiffer rail pads increase the frequency interval where sleeper noise is significant. For frequencies above 1–2 kHz, there is a dominating contribution from wheel vibrations. An experimental procedure to assess rolling noise using a full-scale test rig is described by Hartung and Vernersson [2]. With reasonable accuracy, it can be argued that there is a linear relationship between sound power level and total roughness level [3,4]. The total roughness level is obtained by energetically adding the wheel and rail roughness levels.

Wheel polygonalization may cause severe damage to wheelset and track components. Another type of wheel irregularity is surface or subsurface initiated cracking due to rolling contact fatigue. In this case, a part of the wheel tread may flake off, or a crack may propagate inwards to cause a complete failure of the wheel. For a survey of different wheel irregularities, see Johansson [5]. Causes of periodic wheel (and rail) irregularities and proper countermeasures are surveyed by Nielsen et al. [6]. Damage due to fatigue cracking is discussed by Ekberg and Kabo [7].

The present investigation was initiated since typical levels of different wheel irregularities occurring in Swedish traffic were not known. An investigation, similar to this one, had been performed earlier in The Netherlands by Dings and Dittrich [3]. In the autumn of 2002, an extensive measurement campaign was therefore launched in Sweden. Railway wheels used in freight, commuter (Regina), passenger (X2 and intercity trains) and underground (C20) traffic were investigated. Both tread and disc braked wheels were measured. The randomly selected wheels had travelled a distance of more than 100000 km, and the measurements were conducted when the train wagons/coaches had been taken out of traffic for maintenance, most of them for reasons other than wheel OOR. In total, 99 wheels were measured in order to obtain a representative indication of OOR existing in current traffic in Sweden. The only requirement used in the selection process was the minimum travelled distance of 100000 km.

The measured data were obtained by using mechanical contact measurement methods. Wheel irregularities were measured around the complete wheel circumference at three lateral positions on the tread: the nominal contact position and 10 mm to each side of this position [8]. Magnitudes and wavelength contents of measured wheel OOR are compared with corresponding measurements of rail roughness, obtained by using the method described by Grassie et al. in Ref. [9]. The change in transverse profile due to wear and plastic deformation was studied. Measurements were also performed to determine the hardness of the wheel tread.

2. Description of the measured wheel types

A summary of the measured wheel types is given in Table 1. It was decided to investigate wheels from two types of freight bogies. The Y25 bogie is considered as a "stiff" bogie concerning motion in the lateral and longitudinal directions, whereas the G66 bogie is more flexible. Both bogie types have only primary suspension, i.e. no secondary suspension. On the freight wagons, the so called 2Bgu tread brakes are used. This means that from opposite sides of the wheel, two brake blocks are pressed on to the wheel tread. For passenger train wheels, only one brake block is used and it is pressed on to one side of the wheel (so-called 1Bg tread brake). Cast iron blocks are used for all the (tread braked) wheel categories except for C20, where composite blocks are used.

For powered X2 and C20 wheelsets, most of the braking is applied using disc brakes and/or dynamic brakes (electric braking using the traction motor), whereas a so called scrubber brake is designed to keep the wheel tread clean and to remove some irregularities.

In total, 99 wheels were measured. The numbers of wheels within the categories presented in Table 1 are: C20 new (4), C20 worn (5 + 15), powered X2 (10), trailer X2 (5), tread braked passenger (6), disc braked passenger (6), Regina (12), G66 freight (14) and Y25 freight (22). Worn C20 wheels were measured on two different occasions.

For C20 wheels, a polygonalization problem was known before the start of the measurement campaign. Therefore, a number of trains/wheelsets with known large irregularities were selected. The requirement on travelled distance (100000 km) was also fulfilled in these cases. In addition, recently manufactured wheels were measured in order to study initial irregularities. These selection rules mean that the results presented may not be representative for the whole fleet of C20 trains.

3. Description of the measurement procedures

Three different measurement techniques were used in the investigation of wheel OOR, transverse wheel profile and surface hardness. All three methods are based on mechanical contact between the measuring probes and the wheel surface, followed by subsequent analyses of measured data.

Table 1
Summary of properties of the wheels measured in the campaign

Wheel	Nominal diameter (mm)	Brake type	Bogie type	Train speed [km/h]	Axle load [tonnes]	Traffic type
C20 new	780	Dynamic/scrubber	Powered	80	9.9/12.5	Underground
C20 worn	780	Dynamic/scrubber	Powered	80	9.9/12.5	Underground
X2	1100	Disc/dynamic/ scrubber	Powered	200	18.8	Intercity
X2	880	Disc	Trailer	200	13.6/18	Intercity
Passenger	1020	Block	MD80 (Trailer)	160	16	Intercity
Passenger	920	Disc	ASEA 84S (Trailer)	160	16	Intercity
Regina	840	Disc	Powered	200	18	Commuter traffic
Freight	920	Double block	G66	100	22.5	Freight traffic
Freight	920	Double block	Y25	100	22.5	Freight traffic

The values for train speed and axle load are the allowed maxima. Each row in the table is treated as one category when analyzing the measured data. The nominal diameter is the diameter of a new wheel. For the C20 axle loads, the lower value is for the end bogies, while the higher value is for the middle bogies. A C20 train unit with three coaches has in total four bogies.

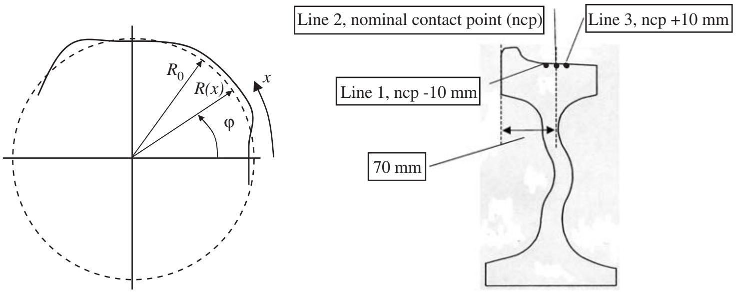

(a) (b)

Fig. 1. (a) Principle sketch of wheel and measurement variables. Radial profile $R(x)$, mean wheel radius R_0, circumferential distance x and corresponding angle φ. The deviation from the mean radius, $r(x) = R(x) - R_0$, is measured. (b) Positions of OOR measurement probes on the wheel tread.

Fig. 2. Out-of-roundness measurement on a powered Regina wheelset.

Three probes in mechanical contact with the wheel tread measured the deviation from the mean radius, $r(x) = R(x) - R_0$, see Fig. 1(a). The centre probe was positioned at the nominal contact point (ncp) 70 mm from the flange side of the wheel, see Fig. 1(b). The other probes were positioned 10 mm to each side of the nominal contact point with Line 1 (probe 1) always positioned closest to the flange side of the wheel. The wheel was rotated by hand approximately two revolutions with the same circumferential starting position for both the left and the right wheel in the wheelset. The deviations from the nominal radius were registered by the probes and stored on a portable computer (Fig. 2). The measurement method has a sampling distance of 0.5 mm and an amplitude resolution of 0.06 μm [8]. The equipment is shown in Fig. 2. The technique requires that the wheelset is lifted, and that the brakes are released, so that the wheelset can be rotated freely.

The transverse profile was measured by use of the MiniProf equipment and the hardness was measured using the EquoTip (EQUO—Energy-QUOtient) equipment. For all wheels, the transverse profile and hardness were measured at the circumferential starting point of the OOR measurement. For some selected C20 wheels, measurements were performed at several positions around the circumference of the wheel. The selected positions corresponded to maxima and minima of the measured OOR. The hardness measurements were performed at the same lateral positions as the OOR measurement lines. For each hardness measurement position, three measurements were performed (at slightly different positions) to enable a calculation of a mean value for a statistically more correct value.

4. Analysis of measured OOR data

In this section, the analysis methods of the measured data will be described. The OOR analyses were performed by ØDS using the software LabView, although similar results were obtained at Chalmers using the same raw data and Matlab. The OOR (raw data) was analyzed to obtain: (i) roughness levels and (ii) harmonic OOR order levels.

4.1. Roughness levels

From the measurements, the roughness/irregularity $r(x)$ [m] was obtained as a function of the circumferential coordinate x [m], see Fig. 1(a). The roughness level L_r^k is defined by

$$L_r^k = 10 \times \log_{10}\{\tilde{r}_k^2/r_{\mathrm{ref}}^2\} \quad [\mathrm{dB\,re\,1\,\mu m}]. \tag{1}$$

Here $\tilde{r}_k^2$ [m^2] is the mean square value of the roughness profile $r(x)$ [m] evaluated in one-third octave band k with centre wavelength

$$\lambda_k = 0.01 \times 10^{k/10}\,[\mathrm{m}], \quad k = -10, -9, \ldots, 14, 15\,[\mathrm{dimensionless}]. \tag{2}$$

Amplitudes for different wavelengths were determined by the discrete Fourier transform (DFT). The squares of the amplitudes of the resulting narrow band spectrum were then summed and multiplied by the factor 1/2 to obtain the mean square value ($\tilde{r}_k^2$ [m^2]) in each one-third octave band. A windowing technique (Tukey, cosine-tapered window) was used together with a number of overlapping DFTs of the same signal. Pits and spikes were removed from the raw data using an algorithm similar to the one described by Dings and van Lier [10]. Using the definition of roughness level L_r^k, an effective roughness amplitude (root-mean-square, rms, value) of 10 μm gives a roughness level of 20 dB, whereas 1 μm corresponds to 0 dB.

4.2. Harmonic OOR order levels

To obtain the contributions to the irregularity from different harmonic orders $\theta = 1,2,3,\ldots$ [dimensionless] of the OOR, the DFT was used. However, the length of the measured signal was now chosen as one wheel revolution to give wavelengths corresponding exactly to the OOR orders that are defined by $\lambda_\theta = 2\pi R_0/\theta$ [m]. Here R_0 [m] is the mean wheel radius obtained from the OOR measurements. The results from the order analysis are presented as rms-values, i.e. $\tilde{r}_\theta = \hat{r}(\lambda_\theta)/\sqrt{2}$ [m], where $\hat{r}$ is the amplitude obtained by the DFT. Further details on the measurement procedures and the analyses of measured data are given in Ref. [11].

5. Results and discussion

In this section, some results are presented for the different types of wheels included in the investigation.

5.1. Out-of-roundness

The results from the OOR measurements are presented as raw data, harmonic order (irregularity) levels and roughness levels (one-third octave band spectra). For the irregularity spectra, orders 1–20 have been determined, corresponding to wavelengths in the interval 120 mm–3.46 m depending on wheel diameter. For the roughness spectra, centre wavelengths ranging from 1.6 to 315 mm are included. The irregularity- and roughness- spectra are thus overlapping in some sense. However, it should be observed that for the roughness spectra, contributions from several wavelengths in each one-third octave band have been summed.

Examples of results for a G66 freight train wheel are presented in Fig. 3. The upper graph presents measured raw data. The different lines (almost coincident in the upper graph) represent the different measured positions, with "Line 1" being closest to the flange for all the wheels. The middle graph presents the irregularity spectrum, i.e. wavelength decomposition into different OOR orders. The first order corresponds to an eccentricity of the wheel, the second to an ovality, etc. The lower graph presents the roughness spectrum.

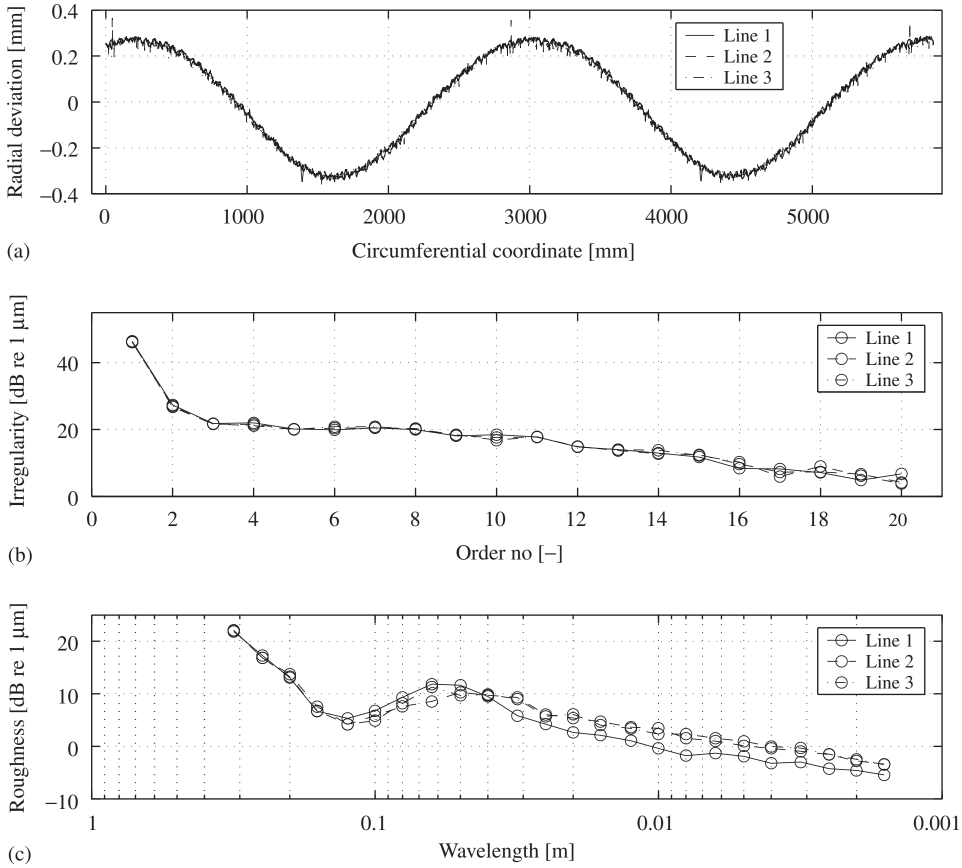

Fig. 3. Examples of measured OOR results for a G66 freight train wheel (two wheel revolutions): (a) raw data, (b) irregularity spectrum and (c) roughness spectrum. The three lines in the upper graph (a) are almost coincident.

From these graphs it can be seen that this particular freight train wheel suffers from a large eccentricity and high roughness levels for wavelengths in the interval 30–80 mm.

The results from several different wheels of the same type, and from different probe positions, have been averaged energetically. This means that the roughness levels $L_{r,n}^{k}$ [dB re 1 μm] were converted into mean square values $\tilde{r}_{k,n}^{2}$ [m^2] (one-third octave band k [dimensionless], wheel number n [dimensionless]), arithmetic mean evaluated (i.e. $\tilde{r}_{k,\mathrm{mean}}^{2} = (1/N)\sum_{n=1}^{N}\tilde{r}_{k,n}^{2}$ [m^2]), and then transformed back to roughness levels ($\bar{L}_{\mathrm{r}}^{k}$ [dB re 1 μm]). The energetic averaging of results from the lateral measurement positions is justified by the size of the wheel–rail contact patch and its lateral motion during vehicle–track/wheel–rail interaction. Energetically averaged results for the different wheel categories are shown in Figs. 4–7. In Fig. 7, also maximum and minimum measured values have been included. For comparison with reported roughness levels, the curve according to prEN ISO3095 [12], has been included as a dashed line. This curve defines a proposed limit for rail roughness in the case of acoustic type testing of new vehicles, representing a very smooth rail. Note that the *total* roughness level spectrum is obtained by energetically adding wheel and rail roughness levels, i.e. summing mean square values of wheel and rail roughness in each one-third octave band.

5.1.1. New and worn C20 wheels

For new C20 wheels, see Fig. 4, there are large contributions from orders 1–4, 6 and 9 to the total irregularity. On these new wheels, the three equidistant positions where the wheel was clamped during the manufacturing were marked. Comparison with the OOR measurements (raw data) indicates that the three minima in the OOR correspond to the clamping positions, which leads to the conclusion that initial

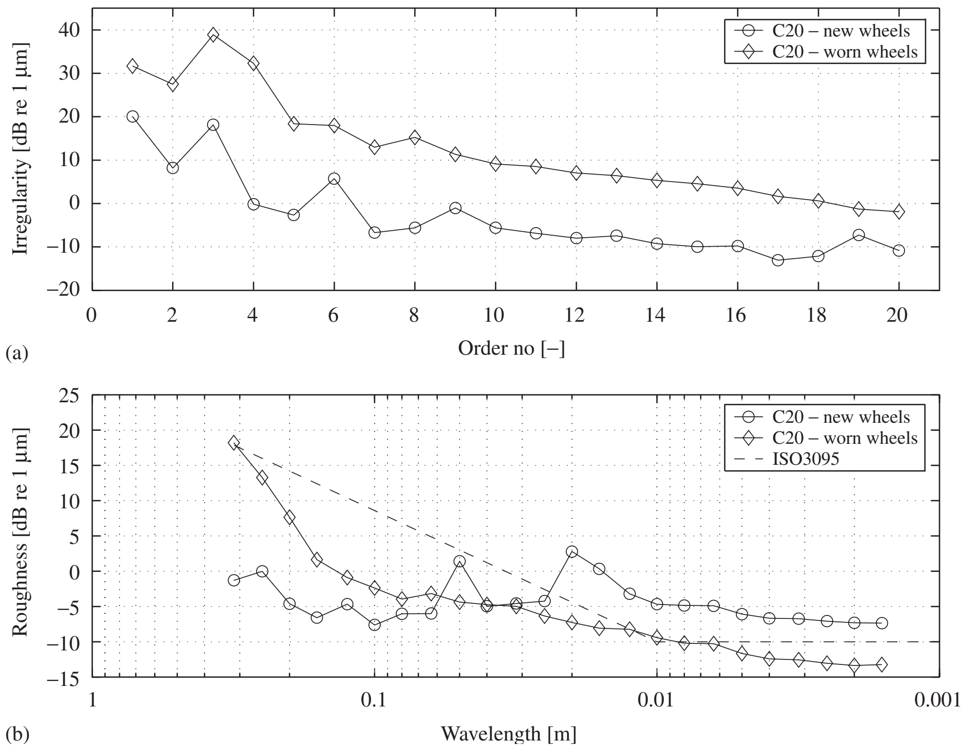

Fig. 4. Comparison of results for new and worn C20 wheels: (a) irregularity spectrum and (b) roughness spectrum.

irregularities are formed due to the clamping in a three-jaw chuck. After turning, when the clamping loads have been released, the wheel rim returns to its undeformed shape causing minima in the initial irregularity to be formed at the three clamping positions around the circumference of the wheel. From the measured data, it is also observed that the lowest levels in the irregularity spectrum are found for the line closest to the flange. This is in accordance with the production technique at Lucchini, where the wheels are clamped on the field side during the last phase of the profiling.

Studying the irregularity spectra for worn C20 wheels in Fig. 4, it is observed that the irregularity contains the largest contributions from orders 1–8. From the measured data it was also observed that the highest harmonic order levels for worn C20 wheels are approximately the same for all three lines. Compared with worn wheels, roughness levels are higher for new wheels for wavelengths shorter than 30 mm. The cause of the polygonalization on C20 wheels is further discussed in Ref. [5].

5.1.2. *Wheels on tread braked freight trains*

For the two types of freight train wheels investigated, the results are shown in Fig. 5. The results for the two different bogie types G66 and Y25 are rather similar. However, the irregularity and roughness levels are higher for G66. Both types suffer from large eccentricities. For Y25 wheels, there is a significant contribution to the total irregularity from the third harmonic order. In the wavelength interval 30–80 mm, there are high roughness levels, which are caused by tread braking [13].

5.1.3. *Powered and trailer X2 wheels*

In Fig. 5, it can be seen that the mean roughness levels for powered X2 high-speed train wheels are similar in level to, and for some wavelengths even higher than, freight train wheels running at a much lower train speed. The roughness levels are greater than 10 dB re 1 μm in the range 30–80 mm. These high roughness levels are most likely caused by tread braking using the cast-iron scrubber brake. It was found that the scrubber brake is used as a service brake rather than as a scrubber brake only, as was intended in the original design [14]. From

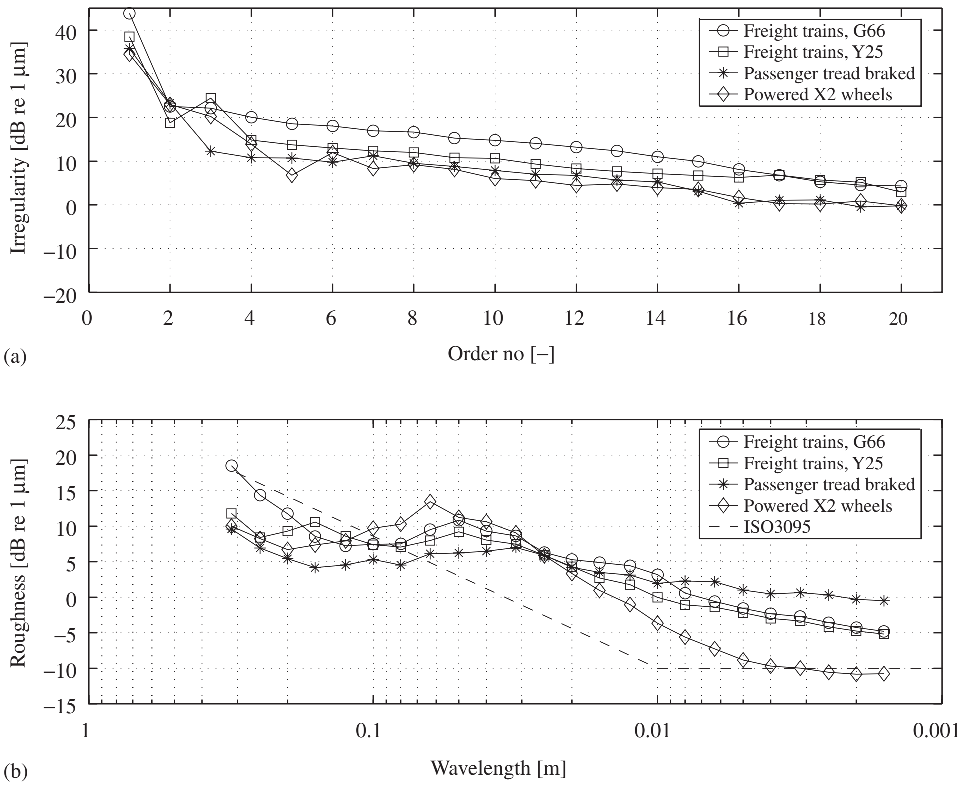

Fig. 5. Comparison of results from freight train wheels, tread braked passenger train wheels and powered X2 wheels: (a) irregularity spectrum and (b) roughness spectrum.

Fig. 6, it is observed that the levels (both irregularity and roughness) are higher for powered wheels than for trailer wheels. According to the roughness spectrum, trailer X2 wheels are smooth, but there is a rather large contribution from the third harmonic order in the irregularity spectrum compared with powered X2 wheels. The roughness levels are low (for both wheel types) for wavelengths shorter than 5 mm.

5.1.4. *Trailer wheels on tread/disc braked passenger trains*

For the tread braked passenger train wheels presented in Fig. 5, there are high roughness levels without appearance of any local maxima. The roughness results for disc braked passenger train wheels, presented in Fig. 6, show high levels for the one-third octave bands 8–25 and 50–150 mm. However, from a closer inspection of the results, it was evident that the two peaks in the roughness spectrum arise mostly due to large contributions from only two of the six measured wheels in the category. The high roughness levels for the wavelength interval 8–25 mm are less significant for noise generation, since the effects of these short wavelengths are attenuated due to the size of the wheel–rail contact patch.

5.1.5. *Powered regina wheels*

The results for the Regina wheels, see Fig. 6, show rather high roughness levels for the whole range of wavelengths, but no specific maxima are found.

5.1.6. *Comparison of wheel types*

In Figs. 5 and 6, several types of wheels are compared. Note that:

- The highest levels in the irregularity spectrum are found for freight wheels and worn C20 wheels, whereas the lowest levels are found for X2 trailer wheels for most orders.

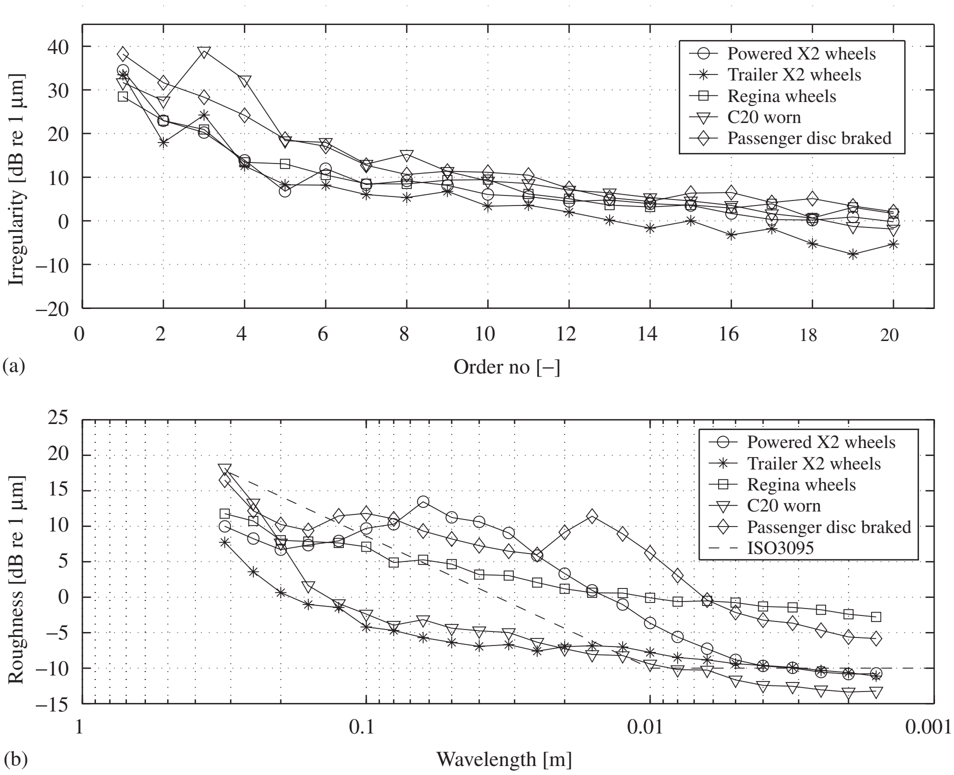

Fig. 6. Comparison of results from X2 wheels, Regina wheels, worn C20 wheels and disc braked passenger train wheels: (a) irregularity spectrum and (b) roughness spectrum.

- All the different wheel types show a rather high eccentricity level (i.e. a high level for order one).
- Depending on wavelength interval, the highest roughness levels are found for either passenger wheels or powered X2 wheels.
- The lowest roughness levels are obtained for X2 trailer wheels (for wavelengths >20 mm) and for worn C20 wheels (for wavelengths <20 mm).

5.1.7. Comparison with measurements of rail roughness

Fig. 7 shows a comparison between rail roughness and wheel roughness for powered X2 wheels. The rail roughness was obtained using the corrugation analysis trolley (CAT) [9] with a sampling distance of 1 mm on UIC60 rails on the main line between Stockholm and Göteborg. Banverket has selected several test sites for monitoring of rail roughness. The chosen positions were based on earlier measurements of wheel–rail contact forces using an X2 train equipped with wheels instrumented with strain gauges. Results from two test sites on a tangent track are shown in Fig. 7, one with a severely corrugated rail and one with a smooth, recently ground rail. The measured distance was 500 m for both rails. From the comparison, it is observed that the maximum roughness levels for powered X2 wheels are similar to roughness levels on a severely corrugated rail. It should be noted that the presented maximum and minimum levels originate from different wheels and that such a worst case scenario (i.e. the maximum values for every one-third octave band or order) has not been measured on one single wheel. The influence of wheel/rail corrugation on rolling contact fatigue in wheels is studied by Nielsen et al. [15].

5.2. Transverse profile

The transverse distribution of wear depth was obtained by subtracting the nominal profile from the worn one, assuming that no wear takes place on the top of the flange. For most of the wheels, there is a weak

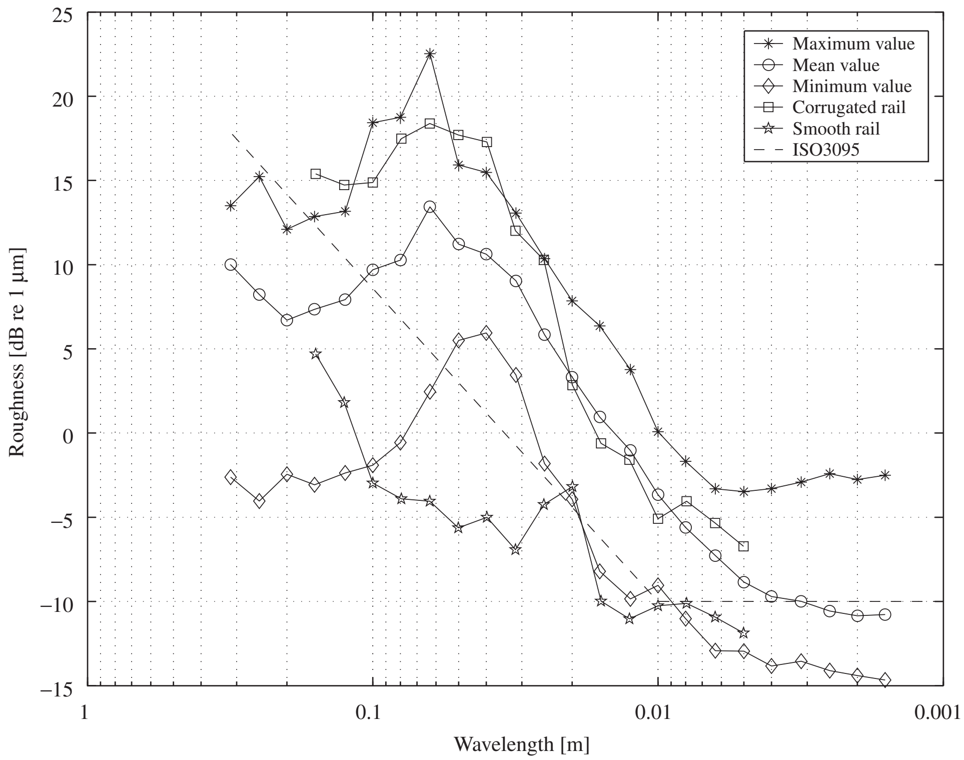

Fig. 7. Comparison between roughness levels from smooth and corrugated UIC60 rails and roughness levels from powered X2 wheels (given as maximum, mean and minimum values). The rail roughness was measured on a section of a Swedish track where high wheel–rail contact forces had been measured earlier using an X2 test train, and on a section with a recently ground rail.

maximum in the transverse distribution of wear depth at approximately 90 mm from the flange side of the wheel. Some exceptions are freight train wheels and Regina wheels, where the amount of wear is fairly constant over the tread. For some of the worn C20 wheels, measurements were performed at several positions around the wheel circumference, corresponding to maxima and minima of the OOR. The wear distribution was found to be similar for these positions, although the magnitude was different corresponding to the maxima and minima due to the OOR. The measurements indicate that the amount of wear is larger for the Y25 bogie than the G66 bogie, although the observed difference may partly be explained by different travelled distances since last reprofiling. This is also in accordance with expectations since the Y25 bogie has a stiffer (lateral and longitudinal) primary suspension than the G66 bogie. Further results from the measurements of transverse profiles are given in Ref. [11].

5.3. *Surface hardness*

The highest hardness values were obtained for tread braked passenger train wheels, while the lowest values were measured on disc braked passenger train wheels. All the values were in the interval 290–390 Brinell. The minimum requirement for hardness 50 mm below the wheel tread for disc braked passenger and X2 wheels is 235 Brinell and 250 Brinell, respectively [16]. Higher hardness values are obtained at the wheel tread due to rim quenching (i.e. heating the wheel and cooling of the wheel tread) during manufacturing. The wheel tread material also hardens during operation. Further results from the measurements of hardness are given in Ref. [11].

6. Concluding remarks

An overview of wheel irregularities occurring in different types of train traffic in Sweden has been given. The previously known polygonalization of underground (C20) wheels was quantified. Freight train wheels and powered X2 wheels had high roughness levels for wavelengths in the approximate range 30–80 mm. The high roughness levels are caused by tread braking using cast-iron brake blocks. High eccentricity levels were found on most of the wheels, with the highest amplitudes for freight wheels. It has been shown that an initial irregularity on new C20 wheels is formed due to the clamping in a three-jaw chuck during profiling. Comparisons of wheel roughness with rail roughness measured on a severely corrugated rail and a smooth, recently ground rail showed that the maximum roughness levels measured on the powered X2 wheels exceeded the levels for the severely corrugated rail. However, the mean roughness spectrum evaluated for 10 such wheels was found to be at a level between the smooth and corrugated rail for most of the wavelengths. To increase the statistical certainty of the presented results, it is recommended to perform more similar measurements, especially on powered X2 wheels and passenger train wheels. With reference to the measured high roughness levels on powered X2 wheels, the present study shows that the use of the cast-iron scrubber brake as a service brake should be avoided. If the present braking practice is not altered, the maintenance (turning) interval needs to be reduced.

A weak maximum in the transverse distribution of wear depth at approximately 90 mm from the flange side (tread wear) was observed for X2, passenger and C20 wheels. The transverse profiles for polygonal C20 wheels were found to be similar around the wheel circumference.

The hardness values varied between 290 and 390 Brinell. The highest values were found for tread braked passenger train wheels, whereas the lowest values were found for disc braked passenger train wheels. The values obtained are all above the minimum requirements for new wheels.

Acknowledgements

This work was performed at the Department of Applied Mechanics, Chalmers University of Technology in Göteborg, Sweden. It forms part of the activities in the Centre of Excellence CHARMEC (CHAlmers Railway MEChanics, www.charmec.chalmers.se).

The measurements were performed in a collaboration between CHARMEC and Ødegaard & Danneskiold-Samsøe (ØDS). From CHARMEC, Mr. Hans Johansson and Dr. Jens Nielsen took part in the planning and execution of the measurements. Personnel at the following companies/locations (workshops) in Sweden contributed to the measurements: Bombardier Transportation Sweden/Västerås, Banverket/Tomteboda (Stockholm), SweMaint/Norrköping, TrainMaint/Hagalund (Stockholm) and Bombardier Transportation Sweden/Högdalen (Stockholm). The C20 measurements were planned and performed in cooperation with Mr. Magnus Lundgren of Bombardier Transportation Sweden. Mr. Jan Spännar of the Swedish National Rail Administration (Banverket) provided the measured rail roughness data. The project was supervised by Dr. Jens Nielsen of Chalmers Applied Mechanics. Professor Roger Lundén gave valuable comments on the manuscript.

References

[1] D.J. Thompson, C.J.C. Jones, A review of the modelling of wheel/rail noise generation, *Journal of Sound and Vibration* 231 (3) (2000) 519–536.

[2] C.F. Hartung, T. Vernersson, A full-scale test rig for railway rolling noise—simulation and measurements of dynamic wheelset–track interaction, *Journal of Sound and Vibration* 267 (3) (2003) 549–563.

[3] P.C. Dings, M.G. Dittrich, Roughness on Dutch railway wheels and rails, *Journal of Sound and Vibration* 193 (1) (1996) 103–112.

[4] D.J. Thompson, On the relationship between wheel and rail surface roughness and rolling noise, *Journal of Sound and Vibration* 193 (1) (1996) 149–160.

[5] A. Johansson, Out-of-round Railway Wheels—causes and consequences, an investigation including field tests, out-of-roundness measurements and numerical simulations, Dortoral Dissertation, Department of Applied Mechanics, Chalmers University of Technology, Göteborg, Sweden, 2005.

[6] J.C.O. Nielsen, R. Lundén, A. Johansson, T. Vernersson, Train–track interaction and mechanisms of irregular wear on wheel and rail surfaces, *Vehicle System Dynamics* 40 (1–3) (2003) 3–54.

[7] A. Ekberg, E. Kabo, Fatigue of railway wheels and rails under rolling contact—an overview, *Wear* 258 (7–8) (2005) 1288–1300.

[8] Ødegaard & Danneskiold-Samsøe (ØDS), A presentation of the company on the web address www.odegaard.dk, 2004.

[9] S.L. Grassie, M.J. Saxon, J.D. Smith, Measurement of longitudinal rail irregularities and criteria for acceptable grinding, *Journal of Sound and Vibration* 227 (5) (1999) 949–964.

[10] P. Dings, S. van Lier, Measurement and presentation of wheel and rail roughness, in: *Proceedings of the Third World Congress on Rail Research (WCCR 1997)*, Florence, Italy, 1997, 10pp.
[11] A. Johansson, Out-of-round railway wheels—measurements of out-of-roundness, transverse profile and surface hardness, Research Report 2004:1, Department of Applied Mechanics, Chalmers University of Technology, Göteborg, Sweden, 2003, 40pp.
[12] CEN/TC256, Railway applications—acoustics—measurements of noise emitted by railbound vehicles, Preliminary European Norm prEN ISO 3095, September 2003, 35pp.
[13] T. Vernersson, M. Petersson, M. Hiensch, Thermally induced roughness of tread braked railway wheels, in: *Proceedings of the 12th International Wheelset Congress*, Qingdao, China, 1998, 8pp.
[14] J. Ågren, Bombardier Transportation Sweden, personal communication, 2004.
[15] J.C.O. Nielsen, A. Ekberg, R. Lundén, Influence of short-pitch wheel/rail corrugation on rolling contact fatigue of railway wheels, *Proceedings of the Institution of Mechanical Engineers, Part F: Journal of Rail and Rapid Transit*, 219, 177–187, 2005.
[16] P. Gullers, Interfleet Technology (formerly TrainTech Engineering Sweden), personal communication, 2004.